Colloids and Surfaces B: Biointerfaces 143 (2016) 318–326

Contents lists available at ScienceDirect

Colloids and Surfaces B: Biointerfaces

journal homepage: www.elsevier.com/locate/colsurfb

Plant plasma membrane aquaporins in natural vesicles as potential stabilizers and carriers of glucosinolates

Maria del Carmen Martínez-Ballesta[a], Horacio Pérez-Sánchez[b], Diego A. Moreno[c], Micaela Carvajal[a,*]

[a] Plant Nutrition Department, Centro de Edafología y Biología Aplicada del Segura (CEBAS-CSIC), Campus de Espinardo, 30100 Murcia, Spain
[b] Bioinformatics and High Performance Computing Research Group (BIO-HPC), Universidad Católica San Antonio de Murcia (UCAM), 30107 Murcia, Spain
[c] Food Science and Technology Department, Centro de Edafología y Biología Aplicada del Segura (CEBAS-CSIC), Campus de Espinardo, 30100 Murcia, Spain

ARTICLE INFO

Article history:
Received 3 February 2016
Received in revised form 15 March 2016
Accepted 18 March 2016
Available online 22 March 2016

Keywords:
Aquaporins
Broccoli
Plasma membrane vesicles
Glucosinolates
Glucoraphanin

ABSTRACT

Their biodegradable nature and ability to target cells make biological vesicles potential nanocarriers for bioactives delivery. In this work, the interaction between proteoliposomes enriched in aquaporins derived from broccoli plants and the glucosinolates was evaluated. The vesicles were stored at different temperatures and their integrity was studied. Determination of glucosinolates, showed that indolic glucosinolates were more sensitive to degradation in aqueous solution than aliphatic glucosinolates. Glucoraphanin was stabilized by leaf and root proteoliposomes at 25 °C through their interaction with aquaporins. An extensive hydrogen bond network, including different aquaporin residues, and hydrophobic interactions, as a consequence of the interaction between the linear alkane chain of glucoraphanin and Glu31 and Leu34 protein residues, were established as the main stabilizing elements. Combined our results showed that plasma membrane vesicles from leaf and root tissues of broccoli plants may be considered as suitable carriers for glucosinolate which stabilization can be potentially attributed to aquaporins.

1. Introduction

During the last few years, membrane vesicles derived from diverse natural sources have received substantial attention as nanocarriers, since they are intrinsically biodegradable and capable of carrying the desired substance to the target cells. Among them, exosomes and differential vesicles have been considered as potential drug-delivery vehicles, since secretion and exchange of cellular contents via extracellular vesicles is a general characteristic of cellular life and a key component in the interaction mechanisms between membranes [1]. Furthermore, advances in genetic engineering tools have contributed to the development of strategies for the use of biologically-derived vesicles as vehicles for the delivery of compounds [2].

Plant-derived vesicles have not been studied for this purpose, but recent results showed cross-reactions between plant and animal membrane [3]. The potential of these natural vesicles with specific lipid/protein composition could be exploited in therapeutic interventions and, in this sense, the use of plant-derived proteoliposomes as drug-delivery systems to target specifically animal cells could be an important feature. However, one of the main problems of the membrane systems is the *in vitro* instability. In previous investigations, we observed that vesicles isolated from plasma membrane and with a high amount of proteins were more stable *in vitro* [4]. Among all the membrane proteins, those that increased to a higher extent as a response of the plants to abiotic stress, such as salinity, were the aquaporins [5].

Aquaporins (AQPs) are transmembrane proteins that belong to the Membrane Intrinsic Proteins (MIP) family and allow the movement of water through biological membranes, bidirectionally. Within the plant, short-distance transport of water and transport in non-vascular tissues occur in part across cellular membranes. Diffusion through the lipid bilayer of these membranes is, however, not sufficient to achieve rapid passage of water and the involvement of aquaporins is necessary to regulate the fine adjustment of membranes permeabilities [6,7], mainly during abiotic stress [8].

The protein activity in biological membranes may depend on the surrounding lipids status. Thus, the effects of binding to non-annular sites on Ca^{2+}-ATPase activity are determined by the nature of the phospholipids surrounding the Ca^{2+}-ATPase (reviewed by Lee [9]). Also, the permeability of the two naturally-occurring isoforms of the aquaporin AQP4, a primary water channel in astro-

* Corresponding author.
E-mail address: mcarvaja@cebas.csic.es (M. Carvajal).

http://dx.doi.org/10.1016/j.colsurfb.2016.03.056
0927-7765/

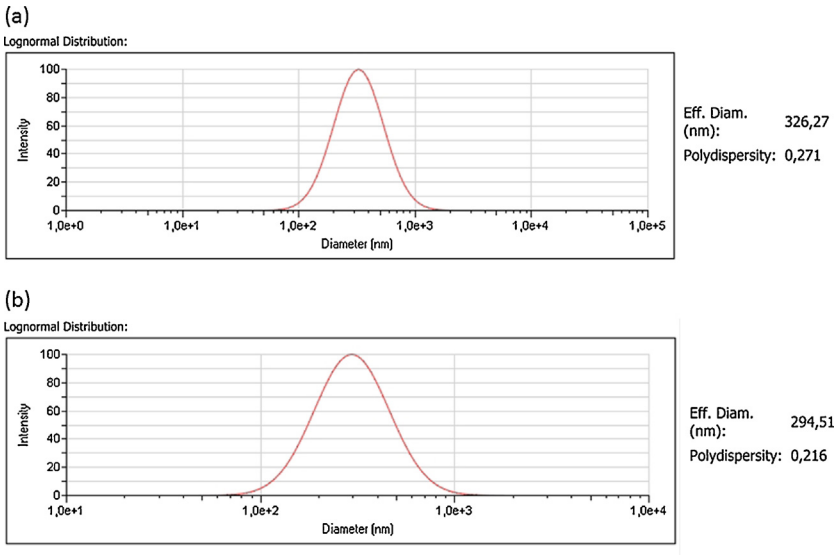

Fig. 1. Average size of plasma membrane vesicles from leaf (a) and root (b). Data are means ± SE (n = 6, n = individual plasma membrane extraction with a protein concentration of 1mg ml^{-1}).

cytes, strongly varied with bilayer composition and decreased with increasing bilayer compressibility modulus and bilayer thickness. These observations suggest that altering the lipid environment provides a means of regulating water channel permeability [10].

The plasma membrane stability of liposomes may be conserved by modifying their surface through the use of hydrophilic polymers such as polyethylene glycol [11]. Also, in solubilization processes, previous to protein reconstitution, the inclusion of polyols (sugar alcohols) together with a mixture of lipids has been shown to protect hydrophobic regions of the protein [12]. The addition of stabilizing agents—such as glycerol, salt, phospholipids, or specific ligands—maintained the integrity of an ATP-binding cassette transporter complex during purification [13]. Based on this, a patented methodology to increase plasma membrane proteins, particularly aquaporins, involving the use of polyol agents as membrane vesicles stabilizers, was established [14].

Glucosinolates are sulfur- and nitrogen-containing secondary metabolites found in the economically-important crops of the Brassicaceae family. They are involved in processes including the induction of resistance against pathogens, control of auxin homeostasis in plants, and prevention of cancer in humans [15,16]. Glucosinolates are water-soluble compounds, found in most plant tissues, that are stable when stored in the vacuoles. They can be hydrolyzed by the enzyme myrosinase to produce isothiocyanates, among other degradation products. Thus, the disruption of plant tissues as a consequence of food preparation, as well as by chewing of vegetables, induces myrosinase release [17]. However, the chemistry of glucosinolates during food processing—and their bioactivity and bioavailability, which enable them to act as beneficial compounds—is complex, depends on numerous factors that influence their stability, and leads to a variety of breakdown products that are also reactive themselves [18].

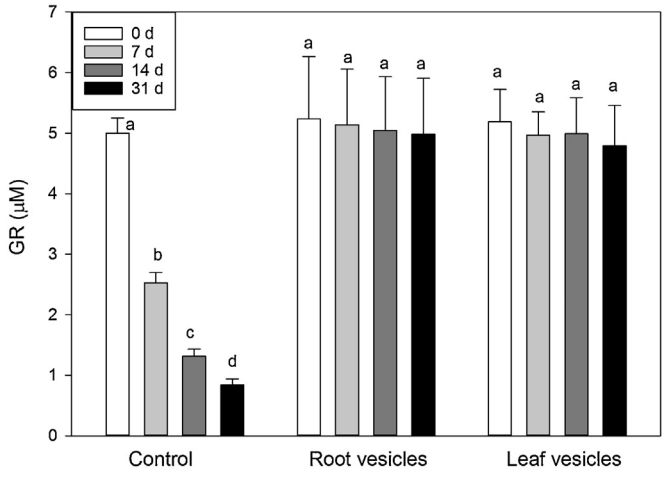

Fig. 2. Concentration (μM) of glucoraphanin (GR) from broccoli seeds in the absence and presence of root and leaf plasma membrane vesicles from broccoli plants, determined at different times (0, 7, 14, and 31 days). Data are means ± SE (n = 6). The same letter indicates no difference ($P > 0.05$, Tukey's test) between treatments.

Different factors may affect and modulate the release of glucosinolates from the natural plant matrix affecting thereby their bioaccesibility and bioavailability by rendering biologically active isothiocyanates (*i.e.* sulphoraphane, SF) and indoles (*i.e.* Indol-3-carbinol) from aliphatic (*i.e.* glucoraphanin) and indolic (*i.e.* glucobrassicin) glucosinolates, respectively [19]. Therefore, it is important to ensure the formation of the desired bioavailable and bioactive metabolite – isothiocyanates – from its precursor glucosinolate in the gastrointestinal tract. However, when purified sulphoraphane is administered, it is rapidly absorbed, metabolized and excreted, with 80% of the intake appearing in the urine within 12–24 h, but the available literature suggests that the percentage of a given dose of glucoraphanin that is delivered SF and excreted is low (30–50%; for review see Angelino and Jeffery [20]). Whether the remaining SF is degraded by microbiota prior to absorption, lost in breath or in feces, or remains bound to amino acids and proteins forming thiourea derivatives and dithiocarbamate esters [21], is not yet fully established, since isothiocyanates are known to be highly reactive and unstable. Therefore, if a major amount of the ingested glucosinolates could reach the colon, where the action of the microbial myrosinase may help in the metabolite transformation and absorption for subsequent absorption through the intestine; with this technique we would have an optimal system for driving the bioavailability of the isothiocyanates during digestion.

In several epidemiological and preclinical studies, different isothiocyanates showed cancer-preventive properties—verifying protective mechanisms of action for these compounds in humans after Brassica vegetable consumption. Isothiocyanates are able to modulate multiple signaling pathways that control processes

such as DNA repair, inflammation, cell growth, apoptosis, and angiogenesis [22]. However, there is no evidence about the Brassica vegetables intake or the Brassica extract dosage necessary to provide isothiocyanate doses equivalent to those that produced effects in *in vitro and in vivo* assays and that may exert similar chemopreventive actions in humans. Therefore, nutritional and pharmacological application of purified glucosinolates could be an advance in the design of new products with functional properties, but adequate stabilization and effective delivery systems for glucosinolates are necessary.

In this work, the osmotic water permeability of proteoliposomes obtained from the root and leaf plasma membrane of broccoli plants was determined in order to study proteoliposomes integrity at different temperatures. Also, glucosinolates self-life stability was assayed in ultrapure water and in the aqueous osmotic buffer (KPB) in which the membrane proteoliposomes are preserved. Glucoraphanin was determined over a time course, in the presence of root and leaf vesicles. A molecular modeling study suggested important interactions, at the atomic level, between aquaporins and the most-efficient glucosinolate in broccoli, glucoraphanin. Thus, a potential binding site for glucoraphanin is proposed, where the main energetic interactions are due to an extended network of hydrogen bonds and partial hydrophobic stabilization. The main residues participating in this interaction have been previously reported in Ref. [23] due to its biological relevance to water channel gating and the support of glucoraphanin stability.

2. Material and methods

2.1. Plant growth

Seeds of broccoli (*Brassica oleracea* L. var. Italica) were pre-hydrated with de-ionized water and aerated continuously for 24 h. After this, the seeds were germinated in vermiculite, in the dark at 28 °C, for two days. They were then transferred to a controlled-environment chamber, with a 16-h light and 8-h dark cycle with temperatures of 25 and 20 °C and relative humidities of 60% and 80%, respectively. Photosynthetically active radiation (PAR) of 400 μmol/m^2 s^{-1} was provided by a combination of fluorescent tubes (Philips TLD 36 W/83, Jena, Germany and Sylvania F36 W/GRO, Manchester, NH, USA) and metal halide lamps (Osram HQI, T 400 W, Berlin, Germany). After five days, the seedlings were placed in 15-L containers with continuously-aerated Hoagland nutrient solution. After two weeks of growth and an osmotic shock (12 dS m^{-1}) applied for one week [14], the roots and leaves were harvested for plasma membrane isolation.

2.2. Plasma membrane isolation and vesicles stabilization

Six different plasma membrane isolations from five plants for each treatment were performed. Root and leaf plasma membranes were purified using the two-phase aqueous polymer technique first described by Larsson et al. [24], and modified by Casado-Vela et al. [25]. Fresh root or third-leaf tissues (20 g) were chopped into small pieces and vacuum-infiltrated with 40 mL of a buffer containing 500 mM sucrose, 10% glycerol, 20 mM Na_2EDTA, 20 mM EGTA, 50 mM NaF, 5 mM β-glycerophosphate, 1 mM 1,10-phenanthroline, 1 mM Na_3VO_4, 0.6% PVP, 5 mM ascorbic acid, 5 mM DTT, and 0.5 mg/L leupeptin in 50 mM Tris-MES, pH 8.0. After buffer infiltration, the tissues were homogenized using a pestle and mortar and filtered through a nylon cloth (240-μm pores). The filtrate was centrifuged at 10,000*g* for 15 min. The supernatant was recovered and centrifuged at 55,000*g* for 35 min, yielding a microsomal pellet which was resuspended in 330 mM sucrose, 2 mM DTT, 10 mM NaF, and 5 mM phosphate buffer (pH 7.8). Plasma membranes were purified from the microsomes by partitioning in a two-phase system mixture with a final composition of PEG-3350 (Sigma)/Dextran-T500 (GE Healthcare), 6.3% (w/w), in the presence of 5 mM KCl, 330 mM sucrose, 2.5 mM NaF, and 5 mM potassium phosphate (pH 7.8) The two-phase system was centrifuged for 5 min at 4000*g*. The resulting upper phase, enriched in plasma membranes, was washed in 9 mM KCl, 300 mM sucrose, 0.2 M EDTA, 0.2 M EGTA, 0.5 M NaF, and 10 mM Tris-borate, pH 8.3, and centrifuged at 55,000*g* for 35 min; the resulting lower phase was resuspended in an appropriate volume of the reported phosphate buffer (pH 6.5) with stabilizing agents (Patent EP12789573.8), to achieve a protein concentration of 2.5 mg mL^{-1}. The protein concentration of the plasma-membrane-enriched fraction was determined with an RC DC Protein Assay kit (BioRad), using BSA as standard. The purity of the plasma membrane preparation was estimated after measuring the enzymatic activities characteristic of the plasma membrane and other organelles [4].

2.3. Size of vesicles

The average size of the vesicles was checked by using light-scattering technology, through intensity measurements with a Malvern ZetaSizer Nano XL machine (Malvern Instruments Ltd., Orsay, France) as previously described in Ref. [26]. This allowed the analysis of particles with sizes ranging from 1 nm to 3 μm.

2.4. Stopped-flow light scattering

The kinetics of the volume adjustment of the membrane vesicles were followed by 90° light scattering at λex = 515 nm. Measurements were carried out at 20 °C in a PiStar-180 Spectrometer (Applied Photophysics, Leatherhead, UK), as described previously in Ref. [27]. Purified membrane vesicles were diluted 100-fold in a buffer containing 30 mM KCl and 20 mM Tris-Mes, pH 8.3 (90 mOsmol kg^{-1} H_2O). Vesicles were mixed with an equal volume of the same buffer used for membrane vesicle equilibration but with a sucrose concentration of 540 mM (630 mOsmol kg^{-1} H_2O). This resulted in a 270 mOsmol kg^{-1} H_2O inward osmotic gradient. The hypo-osmotic shock associated with membrane dilution induced transient opening of the vesicles and equilibration of their interior with the extravesicular solution. The *Pf* was computed from the light-scattering time course according to the following equation: $Pf = k_{exp} V_0/A_v V_w C_{out}$. Where k_{exp} is the fitted exponential rate constant, V_0 is the initial mean vesicle volume, A_v is the mean vesicle surface, V_w is the molar volume of water, and C_{out} is the external osmolarity [27]. For each plasma membrane extraction four Pf measurements were determined for each day and different temperature.

2.5. Lipids analysis

Sterol and fatty acids were determined as described by Chalbi et al. [4]. A mixture of chloroform-methanol (1:2, 0.75 mL) was added in an Eppendorf tube to membranes (0.5 mL), along with β-cholestanol (20 μL, 0.1 mg L^{-1})—used here as an internal standard for sterol analysis. Chloroform ($CHCl_3$; 0.25 mL) was added and the mixture was shaken and centrifuged at 10,000*g* for 6 min. The inter-phase obtained corresponds to the protein content of the membrane. The $CHCl_3$ layer was retained, evaporated to dryness under N_2 (weighing this fraction shows the amount of total lipids), and made up to 100 μL with $CHCl_3$. For sterol analysis, 50 μL of the $CHCl_3$ extract were placed in a glass vial (2 mL), evaporated to dryness under N_2, and acetylated using pyridine (50 μL) and Ac_2O (100 μL). After 2 h, the solvents were evaporated under N_2, ethyl acetate (20 μL) was added, and the sterol analyzed by GC using an HP5-bonded capillary column

(30 m × 0.25 mm × 0.25 μm) coupled to a flame ionization detector (FID), with H_2 as carrier (1 mL min^{-1}) and a temperature program of 120–260 °C at 5 °C min^{-1}, then 260–280 °C at 2 °C min^{-1}, and finally 280–300 °C at 6 °C min^{-1}. The injector and detector temperatures were 150 and 320 °C, respectively. Bound fatty acids were determined by using 50-μL portions of the $CHCl_3$ extract—evaporating them to dryness under N_2, transmethylating with sodium methoxide (0.5 N) in methanol (0.5 mL), and heating at 30 °C for 7 min. The resultant fatty acids methyl esters were extracted with hexane (1 mL), evaporated under N_2, dissolved in ethyl acetate (20 μL), and analyzed by GC using an HP5-bonded capillary column (30 m × 0.25 mm × 0.25 μm), with a FID, He as carrier (1 mL min^{-1}), and a temperature program of 150–195 °C at 3 °C min^{-1}, then 195–220 °C at 2 °C min^{-1}, and finally 220–300 °C at 6 °C min^{-1}. The injector and detector temperatures were 280 and 300 °C, respectively.

2.6. Measurement of glucosinolates stability

Broccoli seeds were washed with sodium hypochlorite (0.5%) and dried in an oven for 24 h at 90 °C. Seeds (40 mg) were ground in a mortar and homogenized by the addition of 750 μL of 70% (v/v) methanol. An equal amount of methanol was added and then the samples were heated at 70 °C for 20 min in a water bath, with a vortex mix every 5 min. The samples were centrifuged at 17,500*g*, at 4 °C, for 15 min. A 1-mL aliquot of the clear supernatant was evaporated using N_2 and the dried residue was reconstituted in ultrapure water or KPB buffer to the initial volume of the supernatant and filtered through a 0.45-μm polyethersulfone membrane filter (Millex HV13, Millipore). The samples were kept on ice during the whole procedure.

Glucosinolates were analyzed according to the procedure described by Dominguez-Perles et al. [28]. Each sample (20 μL) was analyzed in a Waters HPLC-Diode Array Detector (DAD) system (Waters Cromatografía S.A., Barcelona, Spain) consisting of a W600E multisolvent delivery system, in-line degasser, W717 plus autosampler, and W2996 photodiode array detector set at 330 nm. The compounds were separated in a Luna C18 column (25 cm × 0.46 cm, 5 μm particle size; Phenomenex, Macclesfield, UK) with a security guard C18-ODS (4 × 30 mm) cartridge system (Phenomenex). The mobile phase was a mixture of water/trifluoroacetic acid (99.9:0.1, v/v) (A) and acetonitrile/trifluoroacetic acid (99.9:0.1, v/v) (B). The flow rate was 1 mL min^{-1} in a linear gradient, starting with 1% B for 5 min until reaching 17% B at 15 min, which was then maintained for 2 min, then 25% B at 22 min, 35% B at 30 min, 50% B at 35 min, and 99% B at 40 min.

Glucosinolates (227 nm) were eluted off the column at 35 min, identified using a previously-described liquid chromatography–mass spectrometry (LC–MS) method [28], and quantified using sinigrin and glucoraphanin as standards (Phytoplan Diehm & Neuberger, Gmbh, Heidelberg, Germany).

In another set of experiments, glucoraphanin stability was determined by the above method. For this, a glucoraphanin extract (Phytoplan Diehm & Neuberger, Gmbh, Heidelberg, Germany) and vesicles were mixed, reaching a vesicle protein concentration of 0.2 mg mL^{-1} and glucoraphanin concentration of 5 μM. For replications, six measurements from six individual plasma membrane extractions were determined during time after GR addition.

2.7. Glucosinolate-aquaporin binding studies

A blind docking (BD) approach was used to determine to which part of the aquaporin surface glucoraphanin binds. The BD calculations were performed using structural data from a crystal of plant aquaporin obtained from the PDB [29]. The simulations were carried out according to the procedure previously described by Navarro et al. [30], by searching for the global minimum of the potential energy surface with the genetic algorithm implemented in the Lead Finder docking program [31]. The full-atom model of Aquaporin used in the docking calculations was prepared from the raw PDB structure 4IA4. Water molecules were removed and the ionization states of the amino acids were assessed using the Protonate3D function of the MOE software package (Chemical Computing Group, LLC). The same protocol was used to add missing hydrogen atoms in the PDB files, where all charged side chains were considered in their default protonation states at neutral pH. Protein atomic partial charges were derived through the AMBER99 force field [32] implemented in MOE, while the ESP charges were used for glucoraphanin. The size of the grid box for ligand docking was set to 120 Å in each direction from the geometric center of the Aquaporin model. The dG score produced by Lead Finder was taken as the predicted value of the ligand binding energy. The Scoring function of Lead Finder considers the Lennard-Jones term (LJ), metal interactions, solvation term, hydrogen bonds (H-bonds), electrostatic interactions, internal energy of the ligand, contributions to entropy due to ligand torsions, and a solvation penalty term. In this BD approach, multiple docking runs started around the geometric centers of all residues within the selected threshold. A histogram with the resulting distribution of binding energies was obtained, and the pose with the lowest energetic value was selected as the one that had found the most-probable binding spot on the aquaporin surface.

Table 1
Osmotic water permeability (P_f) of root and leaf proteoliposomes over a time course (days), at ambient temperature (25 °C) and at 4 °C. Data are means ± SE (n = 24). The same letter indicates no difference ($P > 0.05$, Tukey's test) between treatments.

Sample Vesicles	Time (days)	P_f (μm s^{-1})25 °C	P_f (μm s^{-1})4 °C
Root	0	11.45 ± 0.12a	14.23 ± 0.33a′
	7	9.21 ± 0.53b	13.56 ± 0.28a′
	14	8.93 ± 0.43b	10.03 ± 0.24b′
	31	8.85 ± 0.62 b	9.95 ± 0.19b′
Leaf	0	21.02 ± 0.87a	24.35 ± 0.84a′
	7	17.79 ± 0.68b	22.87 ± 0.92a′
	14	16.93 ± 0.75b	18,73 ± 0.42b′
	31	15.98 ± 0.63b	17.94 ± 0.63b′

3. Results

3.1. Proteoliposomes size and stability

The size homogeneity of the vesicles was obtained using a Zeta-Sizer Nano XL. The z-average size of the leaf vesicles was 326.27 nm of diameter with a polydispersity index of 0.271, whereas the z-average size of root vesicles was 294.51 nm of diameter with a polydispersity index of 0.216 (Fig. 1). In addition, the stability of the root and leaf proteoliposomes was assayed at ambient temperature (25 °C) and at 4 °C (Table 1). The osmotic water permeability (P_f) was decreased in root and leaf vesicles, relative to the initial values, after 7 days at 25 °C and this was maintained until day 31. However, at 4 °C, the P_f reduction occurred after 14 days. The P_f values were higher in the leaves than in the roots vesicles.

3.2. Chemical composition of the vesicles

The plasma membrane extracted from the leaves and roots of broccoli showed higher percentages of proteins than of lipids (Table 2). However, the protein/lipid ratio of the leaf vesicles was higher than that of the root vesicles. The lipid analysis revealed that both the root and leaf membranes contained a higher percentage of phospholipids (mass%) than of sterols, but the phos-

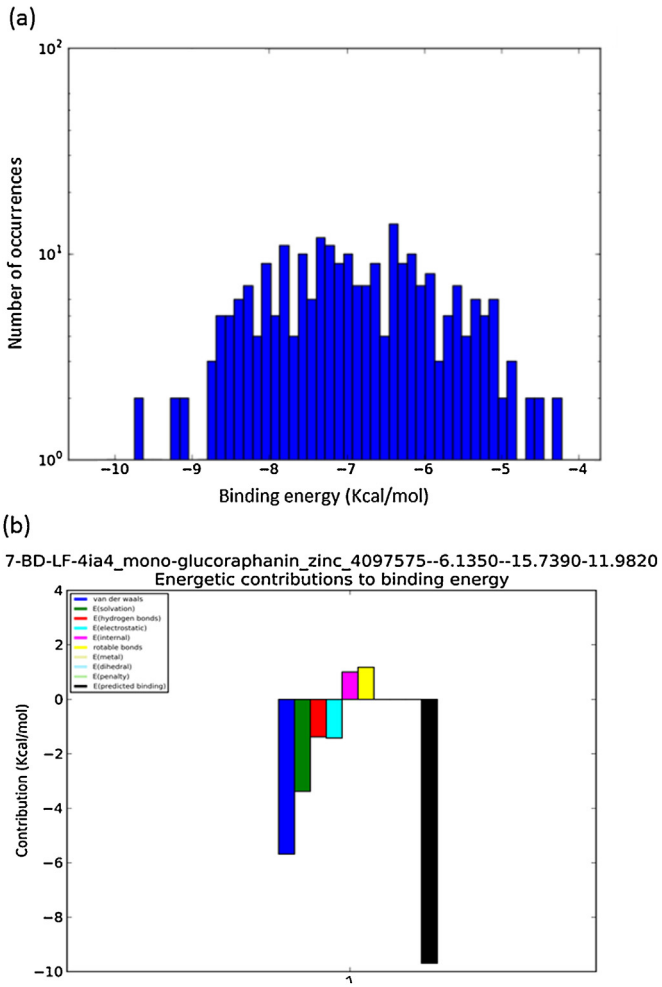

Fig. 3. (a) Histogram obtained from blind docking results. The estimated binding energy (kJ/mol) is shown on the X-axis, while the number of poses or occurrences with binding energy values corresponding to a given interval is shown on the Y-axis. (b) Results for the lowest energy pose obtained from blind docking simulations between glucoraphanin and the plant aquaporin model. The values of the different energetic contributions to the predicted binding energy (kcal/mol) can be observed, the depicted energetic contributions being: van der Waals interactions (deep blue), volume-based free energy of solvation (green), hydrogen bonds (red), electrostatic energy (cyan), energy of entropic losses associated with the ligand's rotatable bonds (yellow), metal interactions (light yellow), dihedral bond energy (light blue), penalty for being outside the grid (light green), and total predicted binding energy (black).

Table 2
Total protein and lipid concentrations of root and leaf plasma membrane vesicles from broccoli plants. The lipid composition was characterized and the phospholipid, fatty acid, and sterol contents in the vesicles were expressed as percentages of the total mass of lipids (n = 6 ± SE, n = individual plasma membrane extraction).

	Roots	Leaves
Total protein (mg mL^{-1})	2.54 (±0.04)	2.51 (±0.06)
Total lipids (mg mL^{-1})	0.84 (±0.01)	0.55 (±0.01)
Parameter	%	%
Phospholipids	**62.3 (±2.53)**	**50.8 (±3.01)**
Fatty acids (FA)		
Palmitoleic (C16:1) (% of Total FA)	41.4 (±1.08)	31.4 (±2.52)
Oleic (C18:1) (% of Total FA)	28.03 (±0.86)	28.03 (±1.88)
Linoleic (C18:2) (% of Total FA)	15.23 (±1.14)	35.23 (±3.01)
Linolenic (C18:3) (% of Total FA)	13.27 (±0.90)	6.27 (±0.83)
Sterols (S)	**21.45 (±2.03)**	**38. 53 (±3.47)**
Brassicasterol (% of Total S)	3.60 (±0. 60)	7.37 (±0.06)
Campesterol (% of Total S)	27.4 (±2.09)	18.42 (±1.09)
Stigmasterol (% of Total S)	45.8 (±3.84)	3.11 (±0.84)
Sitosterol (% of Total S)	23.2 (±1.36)	71.08 (±7.36)

pholipids/sterols ratio was higher in roots than in leaves. According to the fatty acids analyses, in the root plasma membranes palmitoleic acid represented the highest percentage of the total fatty acids, followed by oleic and finally – in a similar proportion – linoleic and linonenic acids. By contrast, in the leaves, the percentages of palmitoleic and linolenic acids were the highest (and similar), followed closely by oleic and then linonenic acid.

The sterols analysis of the plasma membrane (Table 2) showed that there were higher proportions in leaves than in roots. In roots, stigmasterol represented the highest percentage, followed by campesterol, sistosterol, and brassicasterol, while in leaves the percentage of sitosterol was the highest, followed by campesterol, brassicasterol, and stigmasterol.

3.3. *Glucosinolate stability in an aqueous environment*

Different aliphatic (glucoraphanin (GR) and glucoerucin (GE)) and indolic (glucobrassicin (GB), neoglucobrassicin (NGB), and hydroxyglucobrassicin (HGB)) glucosinolates from broccoli seeds were identified in order to study their degradation. The stability of each individual glucosinolate clearly depended on the type of glucosinolate (Table 3). In general, aliphatic glucosinolates were more stable than indolic glucosinolates, at both temperatures studied. Thus, at 25 °C, the GR and GE concentrations were maintained in distilled water and KPB buffer after 1 days. Then, progressive decreases were produced with time, in a similar way in both media,

Table 3
Individual concentrations of aliphatic (GR and GE) and indolic (HGB, GB, and NGB) glucosinolates (μM) from broccoli seeds. Glucosinolate levels were measured over a period of 31 days at ambient temperature (25 °C) and at 4 °C. Data are means ± SE (n = 6, n = individual glucosinolate extraction). The same letter indicates no difference (P > 0.05, Tukey's test) between treatments. (—) No glucosinolates were found.

Time (days)	Solution	Aliphatic glucosinolates 25 °C		Indolic glucosinolates 25 °C		
		GR	GE	HGB	GB	NGB
0	H_2O	4.92 ± 0.05a	1.96 ± 0.05a	1.02 ± 0.02a	0.07 ± 0.00a	0.03 ± 0.00a
	KPB buffer	4.61 ± 0.04a	1.80 ± 0.02a	0.93 ± 0.02b	0.06 ± 0.00a	0.04 ± 0.00a
1	H_2O	4.44 ± 0.03a	1.85 ± 0.02a	0.90 ± 0.02b	0.06 ± 0.00a	0.03 ± 0.00a
	KPB buffer	4.22 ± 0.02a	1.73 ± 0.05a	0.90± 0.01b	0.05 ± 0.00a	0.03 ± 0.00a
7	H_2O	2.65 ± 0.08b	1.36 ± 0.06b	0.67 ± 0.00c	–	–
	KPB buffer	2.88 ± 0.07b	1.22 ± 0.03b	0.70 ± 0.01c	–	–
31	H_2O	1.28 ± 0.08c	1.06 ± 0.03c	–	–	–
	KPB buffer	1.01 ± 0.08c	1.03 ± 0.04c	–	–	–
Time (days)	Solution	Aliphatic glucosinolates 4 °C		Indolic glucosinolates 4 °C		
		GR	GE	HGB	GB	NGB
0	H_2O	4.76 ± 0.03a	1.85 ± 0.03a	0.92 ± 0.02a	0.06 ± 0.00a	0.03 ± 0.00a
	KPB buffer	4.50 ± 0.03a	1.77 ± 0.01a	0.84 ± 0.01a	0.05 ± 0.00a	0.03 ± 0.00a
1	H_2O	4.30 ± 0.04a	1.93 ± 0.01a	1.04 ± 0.03a	0.08 ± 0.00a	0.03 ± 0.00a
	KPB buffer	4.10 ± 0.02a	1.82 ± 0.01a	0.92± 0.01a	0.08 ± 0.00a	0.03 ± 0.00a
7	H_2O	4.09 ± 0.10a	1.89 ± 0.01a	1.00 ± 0.00a	0.08 ± 0.00a	–
	KPB buffer	3.99 ± 0.10a	1.76 ± 0.01a	0.88 ± 0.01a	0.06 ± 0.00a	0.04 ± 0.00a
31	H_2O	4.10 ± 0.03a	1.90 ± 0.03a	1.04 ± 0.02a	–	–
	KPB buffer	4.01 ± 0.08a	1.80 ± 0.02a	1.04 ± 0.02a	0.07 ± 0.00a	0.04 ± 0.00a

the lowest concentrations being reached on day 31. However, GB and NGB were degraded after 7 days of incubation in both media, HGB being the most-stable indolic glucosinolate at this temperature.

At 4 °C, aliphatic glucosinolates were stable in both media, without significant degradation after 31 days. However, indolic glucosinolates were more stable with time in KPB buffer than in distilled water; in the latter, NGB and GB were not detected after 7 days and 31 days, respectively.

Also, to determine the stability of GR, the most important glucosinolate in this cultivar, in the presence of stabilized root and leaf plasma membrane vesicles, the experiments were performed in the modified KPB buffer at ambient temperature, since at 4 °C the glucosinolates were not degraded in the KPB solution (Table 3). Under control conditions (in the absence of vesicles), glucosinolates were increasingly degraded with time (Fig. 2). However, their concentrations were maintained, with respect to the initial values, when root or leaf vesicles were present in the medium.

3.4. Aquaporin-glucoraphanin interaction

From the blind docking calculations for glucoraphanin and aquaporin, detailed information was obtained about the pose giving the highest value for the protein-ligand interaction energy over the entire protein surface Figs. 3–6).

The distribution of the values of the predicted binding energy for all the poses (Fig. 3a) shows that there is one pose that is clearly differentiated from the rest and has a predicted binding affinity value of −9.7 kcal/mol. Quantitative interactions that stabilize or destabilize the binding between the aquaporin and glucoraphanin are shown in Fig. 3b, where the different energetic contributions (kcal/mol) are shown. The main stabilizing interactions were due to Van der Waals forces (a consequence of ligand-protein shape complementarity, blue bar) and solvation (due to hydrophobic stabilization of the linear alkane chain, green bar). Hydrogen bonds and electrostatic interactions (red and blue bars) contributed to a lower degree to the stabilization of the protein-ligand complex, whereas internal ligand energy (magenta bar) and the entropic term (approximated as proportional to the number of rotatable bonds, yellow bar) contributed in the opposite direction to the total binding energy.

Fig. 4 shows that the top pose (pose 1, P1) preferred the part of the outer pore that pointed directly to the intracellular area. There was a second pose (P2), with lower energy, which was predicted to bind to the opposite side of the protein, pointing to the extracellular area. However, the binding energies obtained after P3 were lower; therefore, only two potential binding sites were defined for the aquaporin plant model, P1 being the most probable. Specific residues interacting with the glucoraphanin molecule were observed (Fig. 5). Most of the interactions corresponded to an extended hydrogen bonds network (comprising residues Asp28, Gly30, Phe37, Ser115, Arg118, and His193). Also, stabilization was due to hydrophobic interactions—a consequence of the linear alkane chain of the molecule and the Glu31 and Leu34 residues.

4. Discussion

Biological membranes comprise several interacting components, mainly lipids and proteins. The activity of membrane-

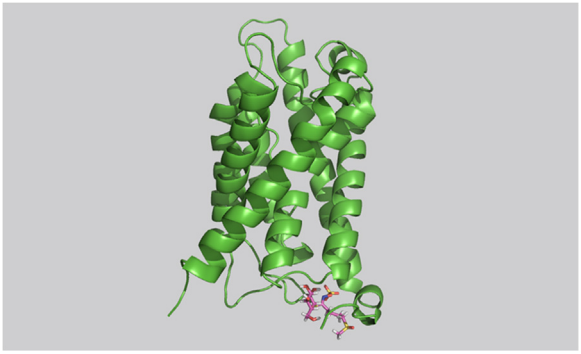

Fig. 4. Top pose (pink skeleton) obtained after blind docking of glucoraphanin with the plant aquaporin model.

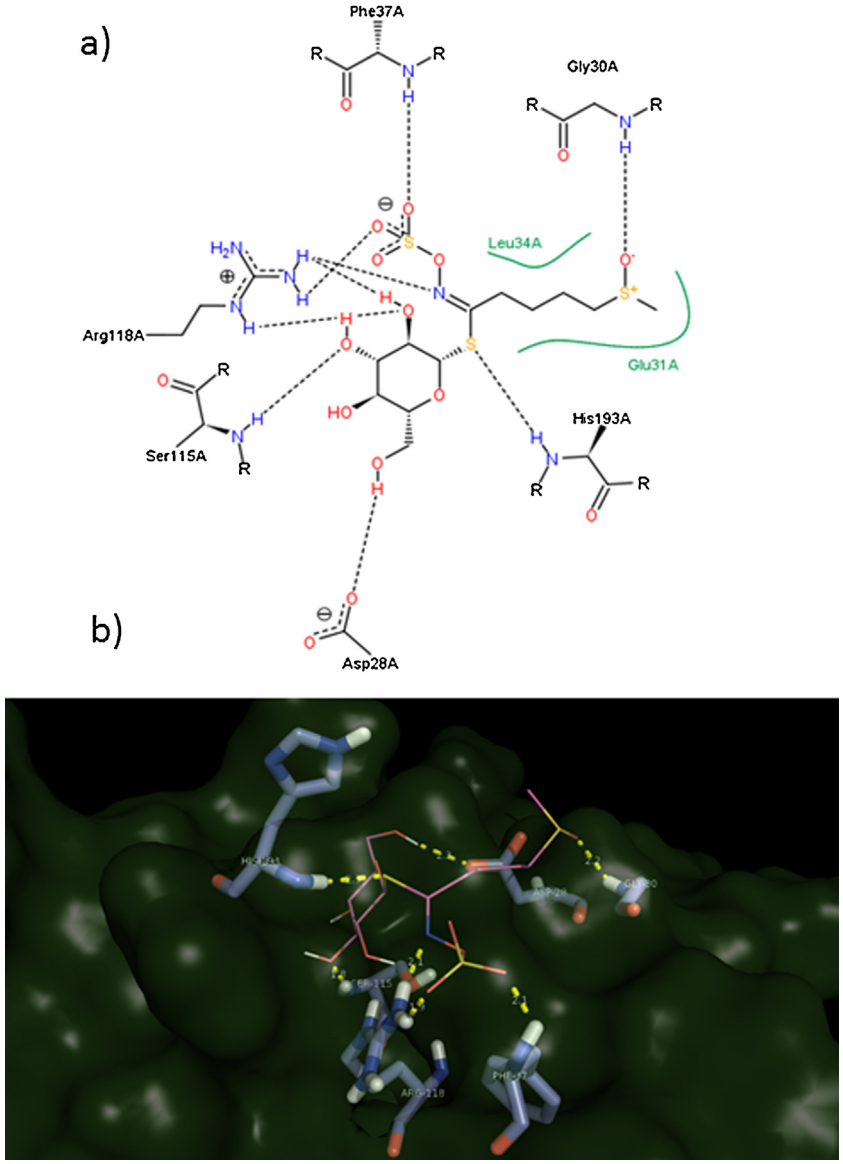

Fig. 5. (a) Detailed representation of the interactions between the top pose of glucoraphanin and aquaporin, obtained after blind docking calculations in two dimensions. Hydrogen bonds are depicted with dashed lines and hydrophobic interactions with green lines. (b) Detailed representation of the interactions between the top pose of glucoraphanin and aquaporin, obtained after blind docking calculations in three dimensions. The most-important hydrogen bonds are depicted with yellow dashes.

associated proteins, such as transporters, may be influenced by the solution environment and its effect on membrane structure [33]. Adequate surfactant agents have been used in functional reconstitutions of a membrane protein to maintain structurally-stable proteoliposomes, since they prevented micelles aggregation and changes in the protein conformation [34]. Polyols are water-soluble substances accepted as lipid vesicle stabilizers and do not need to be removed from the final liposomal product. Therefore, the polyol-influenced chemical properties of our vesicles medium [14], in relation to its use as a stabilizing agent, should explain the maintenance of the P_f values with time—even at ambient temperature. As changes in the protein activity of proteoliposomes, determined by light-scattering spectroscopy, have been demonstrated to be correlated with changes in their structure, P_f conservation in broccoli leaf and root vesicles indicates that not only proteoliposome functionality was preserved, but also the entire structure.

Also, it has been reported that an increase in the osmolality of the external medium induced changes in the lipid bilayer thickness and hydration state of liposomes, thereby modifying the optical properties of dioleoylphosphatidylglycerol (DOPG) liposomes and proteoliposomes [35]. An increase in osmolality due to NaCl addition produced liposome fusion, whereas the use of sucrose avoided liposome aggregation, enhancing the light-scattering intensity [35]. Therefore, in addition to a proteoliposome-stabilization effect, a similar inhibition of vesicles aggregation could be induced by the use of our patented polyol formulation, thus avoiding the P_f reductions with time caused by a vesicle-fusion phenomenon. However, although it must be taken into account that the response to osmotic changes is dependent on vesicle size, in our samples the addition of the stabilization polyol did not affect the size of the vesicles and the extraction process resulted in a standardized size. Also, different P_f values were obtained in vesicles depending on the plant organ (Table 1). The fact that vesicles obtained from leaves had higher P_f could be related to a different lipid and protein composition. A higher protein/lipid ratio in leaves compared with roots probably confers greater membrane stability, as previously reported by Wu et al. [36]. Also, the chemical composition, a high sterol content and fatty acids unsaturation conferring higher water transport

through the membrane bilayer, can account for the *in vitro* membrane stability—as pointed out in Chalbi et al. [4].

Regarding glucosinolate stability, previous studies have reported that the gastric acidity (pH 2.0–3.0) may reduce by up to 60% the content of total glucosinolates in different Brassica cultivars [37]. In Chinese radish, 88–97% of the initial glucosinolate content remained at pH values ranging from 3.6 to 9.1, after incubation at room temperature (23–25 °C) for 2 h, being more stable than at pH < 3.6 [38]. These results are in agreement with our observations, where broccoli seed glucosinolates remained unaltered at pH 6.5 in both pure water and KPB buffer after 1 d. However, the fact that indolic glucosinolates were degraded more rapidly in pure water could be related to the fast hydrolysis of this type of glucosinolate, giving the corresponding isothiocyanate, presumably upon contact with the myrosinase released simultaneously by the seed glucosinolate extraction procedure. A decrease of the solution pH after the addition of ground seeds has been reported in Ref. [39] and the buffer capacity of KPB might be a factor that keeps the pH of the solution steady and higher. In addition, it has been shown that sinigrin and its allyl-isothiocyanate were more stable in soil water than in pure water. Although the substance(s) contributing to the stability were not identified it could be related to the ionic strength of the solution [39].

Thermal breakdown of glucosinolates and their hydrolysis products has been reported in Ref. [40]. The extent of this hydrolysis depends on the type of heat treatment and its duration, the degree of material disintegration, and the vegetable matrix itself [41]. Although most of the work on glucosinolate hydrolysis studied the effect of myrosinase and temperatures as high as 100 °C (cooking temperatures), in our samples —due to the presence of proteins in the vesicles—the thermal treatments were in the range of storage temperatures. However, the fact that a long duration at room temperature was assayed suggests that our vesicles could be used in the food/therapeutic industry to inactivate glucosinolate degradation.

Protein–ligand docking has been employed classically to study the mechanism of interaction of small-molecule AQP inhibitors [42–44], complemented by molecular dynamics (MD) simulations to elucidate the dynamics of the binding of the inhibitor [42,43]. Some of the aquaporin residues predicted in this study have been previously reported in the literature to be involved in important aquaporin-ligand interactions [23]. Thus, the histidine residue His-193 in loop D, which in broccoli corresponds to His–197 at the position equivalent to His-193 in SoPIP2;1 [44], was involved in cytosolic pH-dependent gating in *Arabidopsis* and *Nicotiana tabacum* [45]. Similarly, the N-terminal acidic residues Asp-28 and Glu-31, strictly conserved in PIPs, were involved in both divalent-cation- and H^+-mediated gating [46], these residues being implicated also in the GR-aquaporin hydrogen bonds. Finally, the hydrogen GR-aquaporin binding mode strongly involves other characteristic motifs found throughout the PIP family, such as Ser-115 and Arg-118, located in cytoplasmic loop B, which exist in the putative proteins of PIP1 and PIP2 in broccoli [44]. It has been observed that the Ser-115 residue favors an open-pore conformation and intervenes in aquaporin gating [47].

However, in some cases, a particular inhibitor/activator identified by computational analysis resulted ineffective in subsequent functional experiments. Although some of the residues identified in the GR-aquaporin interaction tighten the closed conformation of the aquaporin, our previous report demonstrated that the addition of exogenous sinigrin, an aliphatic glucosinolate, increased PIP2 aquaporin abundance and functionality in broccoli roots [48]. The mechanism was not characterized but transcriptional regulation was discounted, suggesting aquaporin retention in the plasma membrane due to the sinigrin effect [48]. Whether GR-aquaporin binding blocks or affects aquaporin functionality is not the subject of this work, but it is appropriate for study. Additionally, the structural information about the different binding poses – obtained by docking – might explain the experimental data obtained and the clear GR-aquaporin interaction that stabilizes GR and gives slow and gradual glucosinolate degradation in aqueous solutions. This implies that the predictive capability of the blind docking methodology for the study of GR-aquaporin interactions was accurate.

The fact that GR needs to adopt an unfavorable conformation in order to fit into the aquaporin's binding site is totally compensated by van der Waals interactions, solvation, hydrogen bonds, and electrostatic interactions as the main stabilizing interactions between the glucosinolate and protein. However, the opposite contribution —related to the number of rotatable bonds of the ligand—to the total binding energy was due to the fact that the scoring function used in Lead Finder estimates the entropic contribution to the binding affinity, which is linear versus the number of rotatable bonds. Previously, using the molecular docking technique, the isothiocyanate derived from glucoraphanin, sulforaphane, was shown to bind to human serum albumins via non-polar amino acids [49].

In summary, vesicles have exciting potential applications in the therapeutic/food sectors. A broad range of vesicle types, cells and species of origin, and biogenesis processes should be studied as phytochemical carriers. Promising aspects include the challenge to increase the stability of the vesicles themselves and of the bioactive compound cargo *in vitro* [50]. This new technology fits well into the current knowledge of liposomes and nanoparticles, and great potential exists for engineering new vehicles that combine advantageous elements. The approach presented in this work opens a novel area of investigation: the use of plant vesicles linked to glucosinolates for potential food/therapeutic uses. Also, the results obtained by blind docking show that, according to the plant aquaporin model, GR strongly binds to aquaporin in the proteoliposome, which could be the key to achieving GR stabilization.

Conflict of interest

The authors declare no competing financial interest.

Acknowledgements

The authors thank Dr. E. Barrajón for technical assistance and Dr. D. Walker, for correction of the written English in the manuscript. This work was funded by the Spanish Ministerio de Economía y Competitividad (AGL2012-40175-C02-01). Pérez- Sánchez H has been supported by the Fundación Séneca del Centro de Coordinación de la Investigación de la Región de Murcia under Project 18946/JLI/13 and by the Nils Coordinated Mobility under grant 012-ABEL-CM-2014A, in part financed by the European Regional Development Fund (ERDF).

References

[1] I. Curtis, J. Meldolesi, J. Cell Sci. 125 (2012) 4435.
[2] B. Gyorgy, M.E. Hung, X.O. Breakefield, J.N. Leonard, Annu. Rev. Pharmacol. Toxicol. 55 (2015) 439.
[3] R.A. Vaishnav, R. Liu, J. Chapman, A.M. Roberts, H. Ye, J.D. Rebolledo-Mendez, T. Tabira, A.H. Fitzpatrick, A. Achiron, M.P. Running, R.P. Friedland, J. Neuroimmunol. 260 (2013) 92.
[4] N. Chalbi, M.C. Martinez-Ballesta, N.B. Youssef, M. Carvajal, J. Plant Physiol. 175 (2015) 148.
[5] K. Bernfur, O. Larsson, C. Larsson, N. Gustavsson, PLoS One 8 (2013) e71206.
[6] M.C. Martínez-Ballesta, C. Silva, C. López-Berenguer, F.J. Cabañero, M. Carvajal, Plant Biol. 8 (2006) 535.
[7] C. Maurel, L. Verdoucq, D.T. Luu, V. Santoni, Annu. Rev. Plant Biol. 59 (2008) 595.
[8] B. Muries, M. Carvajal, M.C. Martínez-Ballesta, Planta 237 (2013) 1297.
[9] A.G. Lee, Biochim. Biophys. Acta 1666 (2004) 62.
[10] J. Tong, M.M. Briggs, T.J. McIntosh, Biophys. J. 103 (2012) 1899.
[11] B. Stark, G. Pabst, R. Prassi, Eur. J. Pharm. Sci. 41 (2010) 546.
[12] I. Tetlow, C. Bowsher, M. Emes, Biochem. J. 319 (1996) 717.

[13] E.R. Geertsma, N.A.B.N. Mahmood, G.K. Shuurman-Wolters, B. Poolman, Nature 3 (2008) 256.
[14] M. Carvajal, C. García-Viguera, D.A. Moreno, M.C. Martínez-Ballesta, Patent EP2716280, (2011).
[15] D.J. Kliebenstein, J. Kroymann, T. Mitchell-Olds, Curr. Opin. Plant Biol. 8 (2005) 264.
[16] A.W. Woodward, B. Bartel, Ann. Bot. (Lond.) 95 (2005) 707.
[17] R. Kissen, J. Rossiter, A. Bones, Phytochem. Rev. 8 (2009) 69.
[18] F.S. Hanschen, E. Lamy, M. Schreiner, S. Rohn, Angew. Chem. 53 (2014) 11430.
[19] F.A. Tomás-Barberán, A. Gil-Izquierdo, D.A. Moreno, Designing Functional Foods: Understanding, Measuring and Controlling Food Structure Breakdown and Nutrient Absorption for the Development of Health-promoting Foods. Part 3. Digestion and Adsorption of Food Components, in: D.J. McClemments, E.A. Decker (Eds.), Woodhead Publishing Ltd. CRC Press, Boca Raton, Fl, USA, 2009, p. 194 (ISBN: 978-1-84569-432-6, Chapter 19).
[20] D. Angelino, E. Jeffery, J. Funct. Food 7 (2014) 67.
[21] R. Verkerk, M. Schreiner, A. Krumbein, E. Ciska, B. Holst, I. Rowland, R. De Schrijver, M. Hansen, C. Gerhäuser, R. Mithen, M. Dekker, Mol. Nutr. Food Res. 53 (2009) 1.
[22] B.B. Aggarwal, H. Ichikawa, Cell Cycle 4 (2005) 1201.
[23] A. Frick, M. Järva, S. Törnroth-Horsefield, FEBS Lett. 587 (2013) 989.
[24] C. Larsson, S. Widell, P. Kjellbom, Methods Enzymol. 148 (1987) 558.
[25] J. Casado-Vela, B. Muries, M. Carvajal, I. Iloro, F. Elortza, M.C. Martínez-Ballesta, J. Proteome Res. 9 (2010) 3479.
[26] E. Barrajon-Catalan, M.P. Menendez-Gutierrez, A. Falco, A. Carrato, M. Saceda, V. Micol, Cancer Lett. 290 (2010) 192.
[27] C. Maurel, F. Tacnet, J. Glücü, J. Guern, P. Ripoche, Proc. Natl. Acad. Sci. U. S. A. 94 (1997) 7103.
[28] R. Dominguez-Perles, M.C. Martínez-Ballesta, M. Carvajal, C. García-Viguera, D.A. Moreno, Food Chem. 75 (2010) 383.
[29] J.L. Sussman, L. Dawei, J. Jiansheng, N.O. Manning, J. Prilusky, O. Ritter, E.E. Abola, Acta Crystallogr. Sect. D- Biol. Crystallogr. 54 (1998) 1078.
[30] J. Navarro-Fernandez, H. Pérez-Sánchez, I. Martinez-Martinez, I. Meliciani, J.A. Guerrero, V. Vicente, J. Corral, W. Wenzel, J. Med. Chem. 55 (2012) 6403.
[31] O.V. Stroganov, F.N. Novikov, V.S. Stroylov, V. Kulkov, G.G. Chilov, J. Chem. Inf. Model. 48 (2008) 2371.
[32] J. Wang, P. Cieplak, P.A. Kollman, J. Comput. Chem. 21 (2000) 1049.
[33] J.M. Wood, Microbiol. Mol. Biol. Rev. 63 (1999) 230.
[34] V.L. Gaikwad, M.S. Bhatia, Saudi Pharm. J. 21 (2013) 327.
[35] G.F. White, K.I. Racher, A. Lipski, F.R. Hallett, J.M. Wood, Biochim. Biophys. Acta 1468 (2000) 175.
[36] J. Wu, D.M. Seliskar, J.L. Gallagher, Am. J. Bot. 92 (2005) 852.
[37] F. Vallejo, A. Gil-Izquierdo, A. Pérez-Vicente, C. García-Viguera, J. Agric. Food Chem. 52 (2004) 135.
[38] P. Jing, S.J. Zhao, S.Y. Ruan, Z.H. Xie, Y. Dong, L. Yu, Food Chem. 133 (2012) 1569.
[39] R. Tsao, Q. Yu, I. Friesen, J. Potter, M. Chiba, J. Agric. Food Chem. 48 (2000) 1898.
[40] M. Dekker, R. Verkerk, W.M.F. Jongen, Trends Food Sci. Technol. 11 (2000) 174.
[41] E. Rosa, R.K. Heaney, F.C. Rego, Hortic. Rev. 19 (1994) 99.
[42] F.J. Detmers, B.L. de Groot, E.M. Müller, A. Hinton, I.B. Konings, M. Sze, S.L. Flitsch, H. Grubmüller, P.M. Deen, J. Biol. Chem. 281 (2006) 14207.
[43] E.M. Muller, J.S. Hub, H. Grubmuller, B.L. de Groot, Pflugers Arch. 456 (2008) 663.
[44] B. Muries, M. Faize, M. Carvajal, M.C. Martínez-Ballesta, Mol. Biosyst. 7 (2011) 1322.
[45] C. Tournaire-Roux, M. Sutka, H. Javot, E. Gout, P. Gerbeau, D.T. Luu, R. Bligny, C. Maurel, Nature 425 (2003) 393.
[46] L. Verdoucq, A. Grondin, C. Maurel, Biochem. J. 415 (2008) 409.
[47] M. Fischer, R. Kaldenhoff, J. Biol. Chem. 283 (2008) 33889.
[48] M.C. Martínez-Ballesta, B. Muries, D.A. Moreno, R. Domínguez-Perles, C. García-Viguera, M. Carvajal, Physiol. Plant. 150 (2014) 145.
[49] P. Abassi, F. Abassi, F. Yari, M. Hashemi, S. Nafisi, J. Photochem. Photobiol. B 122 (2013) 61.
[50] K. Winkler, G. Leneweit, R. Schubert, Colloids Surf. B 45 (2005) 57.